Exploiting the Nanoparticle Plasmon Effect: Observing Drug Delivery Dynamics in Single Cells *via* Raman/Fluorescence Imaging Spectroscopy

Bin Kang,[†] Marwa M. Afifi,[‡] Lauren A. Austin, and Mostafa A. El-Sayed*

Laser Dynamics Laboratory, School of Chemistry and Biochemistry, Georgia Institute of Technology, Atlanta, Georgia 30332-040, United States.
[†]Present address: College of Material Science and Technology, Nanjing University of Aeronautics and Astronautics, Nanjing, 210016, People's Republic of China.
[‡]Present address: Department of Oral Pathology, Faculty of Dentistry, Alexandria University, Champillion St, Azarita, Alexandria, Egypt.

ABSTRACT Drug delivery systems (DDSs) offer efficient and localized drug transportation as well as reduce associated side effects. In order to better understand DDSs, precise observation of drug release and delivery is required. Here, we present a strategy, plasmonic-tunable Raman/fluorescence imaging spectroscopy, to track the release and delivery of an anticancer drug (doxorubicin) from gold nanoparticle carriers in real time at a single living cell level. A pH-responsive drug release profile was attained through the conjugation of doxorubicin (DOX) to the nanoparticle surface *via* a pH-sensitive hydrazone linkage. When DOX is bound to the surface of the gold nanoparticle, its surface-enhanced Raman spectrum can be seen, but its fluorescence is quenched. When released, due to the lysosomes' acidic pH, its Raman enhancement is greatly reduced, changing the acquired Raman spectrum and in turn allowing for the visualization of its fluorescence signal. The plasmonic-tunable Raman/fluorescence properties enabled the tracking of the DOX release and delivery process from the gold nanoparticle surface to the lysosomes of single living cells under the acidic pH change of their microenvironments. This technique offers great potential to follow the molecular mechanisms of drug delivery and release in living cells, as well as the cellular response to drug action.

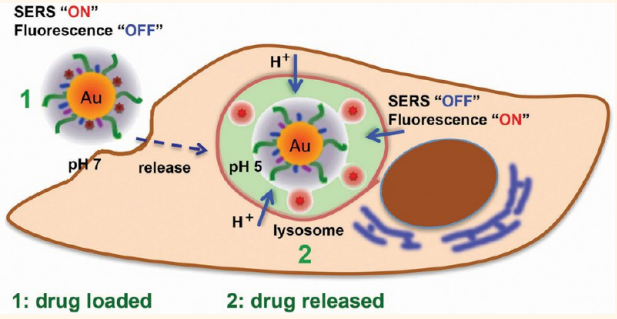

KEYWORDS: plasmonic nanoparticles · fluorescence · Raman · drug release · tracking

Due to their unique optical properties, plasmonic nanoparticles (*i.e.*, gold or silver) have been utilized in a wide range of biomedical applications such as imaging, sensing, and photothermal therapy.[1−4] By utilizing the plasmonically enhanced Rayleigh scattering from gold or silver nanoparticles targeted to specific cell components, it has been possible to obtain the real-time cellular imaging of cancer cells during the complete cell cycle.[5−7] Recently, our group has developed a new technique to simultaneously observe the Rayleigh scattering cellular imaging and the Raman scattering molecular vibration signals from molecules near the nucleus of a single living cell.[8] This technique, named targeted plasmonically enhanced single cell imaging spectroscopy (T-PESCIS), allows monitoring of the cellular and molecular changes throughout an entire cell cycle or until cell death when induced by anticancer drugs.

Drug delivery systems using nanomaterials have been widely utilized to improve drug transportation and drug action, reduce the drug dosage, and minimize drug side effects.[9,10] Gold nanoparticles (AuNPs) are very promising candidates as drug carriers because of their small size, biocompatibility, facile surface modification, and adequate cell penetration.[4] Through the thoughtful design of nanoparticles, drug release can be triggered through internal or external stimuli, such as pH change,[11] light,[12,13] and temperature changes.[14,15] The pH-responsive drug release can be achieved through the conjugation of the drug to AuNPs *via* a pH-sensitive linker.[16] It has been proposed that the drug gets released from the nanoparticles in the lysosomes due to their acidic

* Address correspondence to melsayed@gatech.edu.

Received for review July 1, 2013 and accepted August 2, 2013.

Published online August 02, 2013
10.1021/nn403351z

microenvironment right after being internalized by the targeted cells.[11,16] Understanding the precise mechanism behind drug release from AuNPs is important to improve the current knowledge of intracellular events associated with drug delivery and the design of new controlled drug release systems. Tracking this process in living cells requires the determination of the location and movement of the AuNPs carriers and the drug status (loading or release) simultaneously, which still remains a challenge.

In the present work, we propose a new strategy, plasmonic-tunable Raman/fluorescence imaging spectroscopy (P-TRFIS), to directly track the delivery and release of an anticancer drug from AuNPs in single living cells. A commonly used anticancer drug, doxorubicin (DOX), was conjugated to the surface of AuNPs *via* a pH-sensitive hydrazone linkage to promote pH-responsive drug release. The Raman and fluorescence signals of DOX molecules were selectively switched "ON" or "OFF" by the plasmonic field of AuNPs depending on the distance between the DOX molecules and the AuNPs. Through monitoring the Raman and fluorescence signals of DOX, tracking DOX delivery and release from AuNPs' surface in the lysosomes of single living cells under the acidic pH change of their microenvironments was possible.

RESULTS AND DISCUSSION

Nanoparticle Design and Drug Loading. Gold nanospheres with a diameter of 28 ± 3 nm were synthesized by the citrate reduction method.[17] TEM images and UV−vis spectroscopy confirmed the above-mentioned size and shape (Figure S1). AuNPs were used to load DOX molecules and enhance/quench the Raman/fluorescence signals. The surface of the AuNPs was first modified by polyethylene glycol (PEG) to improve the biostability and reduce nonspecific binding of proteins.[18,19] Following PEGylation, arginylglycylaspartic (RGD) and nuclear localizing signal (NLS) peptides were conjugated to the particle surface to increase internalization of the particles as well as selectively deliver the AuNPs about the cell nucleus.[20,21] Figure 1 illustrates a schematic diagram of the nanoparticles' design for pH-responsive drug release and the tracking principle behind the DOX release in single living cells by the P-TRFIS technique. DOX, a commonly used anticancer drug, was selected as our drug model since it has a red fluorescence emission as well as a strong Raman scattering signal. It was conjugated to the AuNPs through a pH-sensitive hydrazone linkage by methyl thioglycolate and hydrazine (Figure 1a), by the method described previously.[16] The distance between

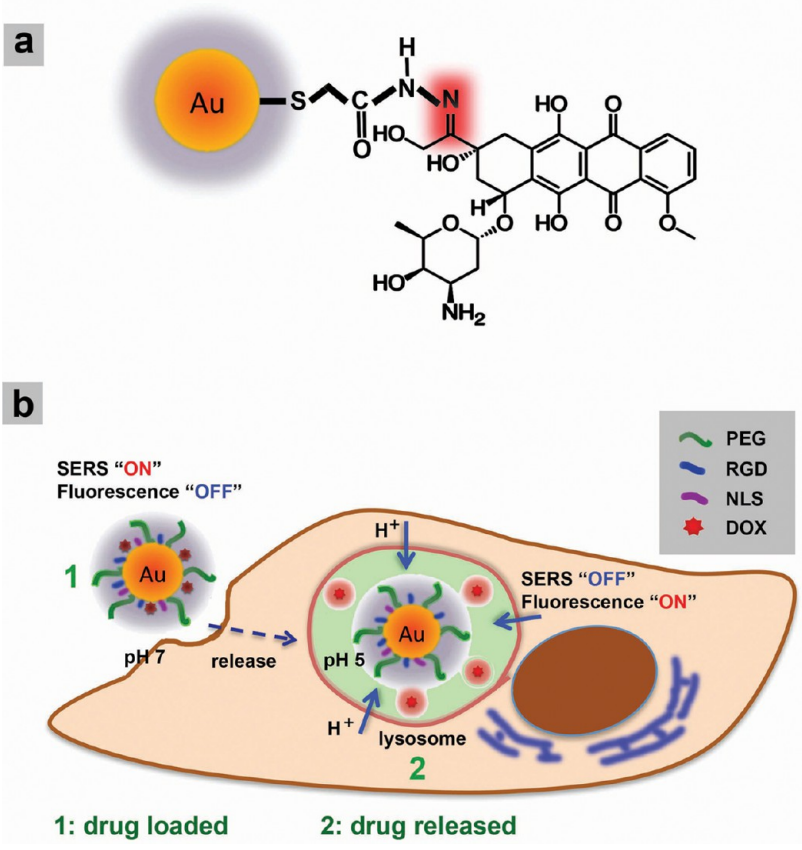

Figure 1. (a) Illustration of the AuNPs functionalized with the anticancer drug doxorubicin (DOX) using a pH-sensitive hydrazine linkage (highlighted in red). (b) Schematic diagram of pH-triggered drug release tracking in acidic lysosomes by monitoring the surface-enhanced Raman spectra (SERS) and fluorescence signal from the DOX molecules.

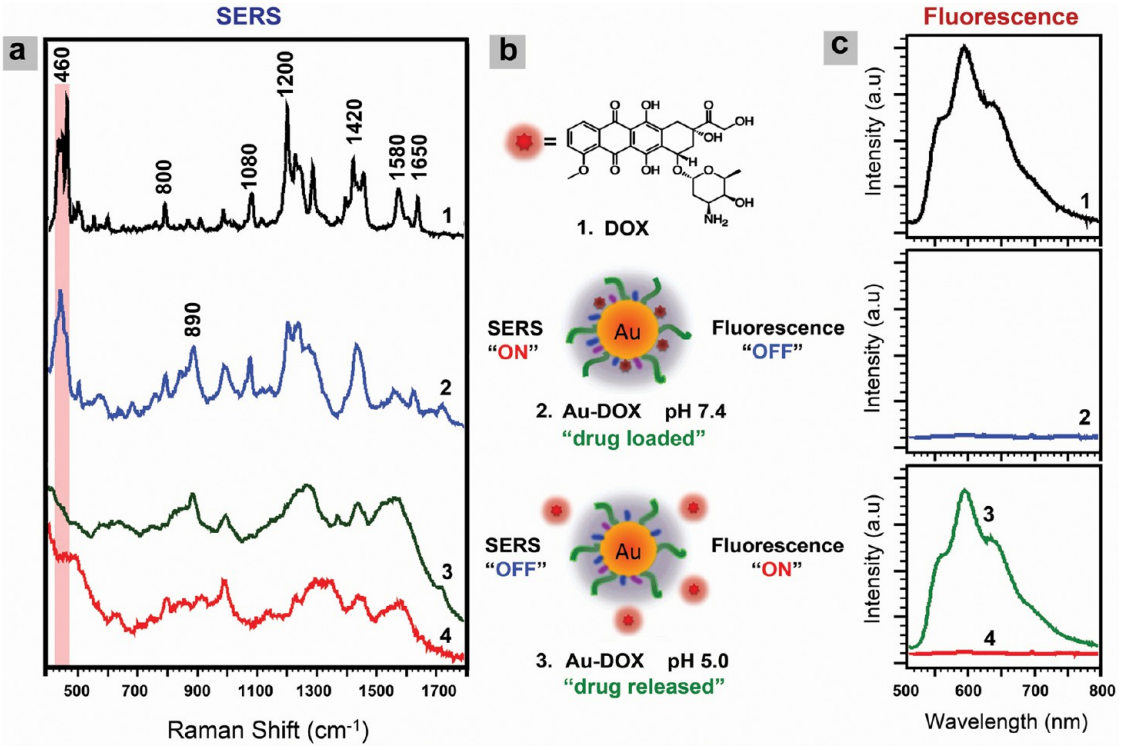

Figure 2. (a) Normal Raman spectrum of free DOX molecules (1) and surface-enhanced Raman spectra (SERS) of DOX bound to AuNPs (2) at pH 7.4, DOX-AuNPs at pH 5.0 (3), and AuNPs without close-by DOX (4). (b) Schematic diagram of the chemical structure of DOX (1), DOX-AuNPs at pH 7.4 (2), and DOX-AuNPs at pH 5.0 (3). (c) Fluorescence spectra of free DOX in solution (1), DOX-AuNPs at pH 7.4 (2), DOX-AuNPs at pH 5.0 (3), and AuNPs without DOX (4).

the DOX molecules and the AuNPs' surface was roughly calculated to be about 1 nm according to the bond distances associated with the linkers.

P-TRFIS Principle. The P-TRFIS technique is based on the selective quenching or enhancement effect of Raman or fluorescence signals by the plasmonic field of AuNPs. The AuNPs tends to quench the fluorescence of molecules when they are closely located to the surface of the AuNPs (<5 nm),[22] while significantly enhancing their Raman signals.[23] On the other hand, increasing the distance between such molecules and the AuNPs surface by 20 nm or more allows the plasmon far field to enhance its fluorescence signal as the nanoparticles are not close enough to the molecules to quench their fluorescence.[24] Consequently, at these distances the molecular Raman signal is not enhanced.

As such, when DOX molecules were conjugated to the AuNPs' surface, the Raman signal of DOX was significantly enhanced by the near-field plasmon of the AuNPs, while the fluorescence signal was quenched. This condition is referred to as the "drug-loaded" state, where the SERS signal is strong and the fluorescence signal is quenched (Figure 1b). When the DOX-loaded gold nanoparticles (DOX-AuNPs) are internalized by cells and transported into the acidic environment of their lysosomes (*i.e.*, pH = 5.0), the hydrazone bond breaks, releasing the DOX molecules from the AuNPs. Once the DOX molecules are detached from the AuNPs and diffused into the cellular environment, the Raman signal of DOX molecules is significantly decreased, since they are out of the plasmonic field of AuNPs, yet their fluorescence signal is recovered. This is named the "drug released" state and corresponds to the "OFF" SERS signal and the "ON" fluorescence signal (Figure 1b). Thus, by monitoring the plasmonic enhancement or quenching of the Raman and the fluorescence intensity from the DOX molecules, it is possible to track the drug release process from AuNPs to the living cells in real time.

***In Situ* Confirmation of P-TRFIS.** The principle of DOX-AuNP design and the P-TRFIS strategy was first investigated in aqueous solution by recording both Raman and fluorescence spectra under different pH conditions. The Raman spectrum of DOX has several strong, sharp bands at around 460, 1200−1300, 1420, 1580, and 1650 cm^{-1} (Figure 2a.1), which correspond to the C═O in-plane deformation, in-plane bending motion of C−O, C−O−H, and C−H, skeletal ring vibrations, and hydrogen-bonded C═O stretching modes, respectively (Table 1).[25−27] After conjugating DOX to AuNPs, the Raman spectrum of DOX-AuNPs was similar to that of free DOX molecules, except that all bands were broadened and some new bands around 800−900 cm^{-1} appeared (Figure 2a.2). Acidic buffer was then added to the DOX-AuNP solution to reduce the pH to 5.0. As a result, most of the Raman bands associated with DOX molecules decreased in intensity

TABLE 1. Assignment for the Main Raman Spectroscopic Bands in Our Systems

	assignment	
band (cm^{-1})	DOX	cell
460	C═O deformation	
500		—S—S—, protein
645		C—S, guanine
838		DNA backbone
1000		phenylalanine
1128		C—N peptide bond
1200—1300	C—O bending	
1300		amide III
1420	C—O—H, C—H bending	
1580	skeletal ring	
1650	C═O stretching	

(Figure 2a.3), but the spectral features still remained similar to those observed when bound to the AuNPs (Figure 2a.4). Since the AuNPs were functionalized with other ligands, such as PEG, RGD, and NLS, the Raman spectrum of AuNPs had several broad bands (Figure 2a.4). When the DOX was loaded onto the particle surface, the Raman signals of DOX molecules were significantly enhanced by their proximity to the surface of gold nanoparticles (Figure 2b.2). The Raman spectra of DOX molecules taken alone and conjugated to AuNPs have several overlapping bands at 1200, 1300, 1400, and 1600 cm^{-1}, indicating these bands should not be used when tracking the drug release process. Thus, the 460 cm^{-1} band was selected to track the loaded *versus* released states of the drug. Figure 2c shows the fluorescence spectra of DOX and DOX-AuNPs recorded at different pHs and an excitation wavelength of 490 nm. The DOX molecules in solution (Figure 2b.1) have an emission band with a maximum at around 600 nm (Figure 2c.1). Once DOX was loaded onto the particle surface (Figure 2b.2), its fluorescence signal was almost completely quenched (Figure 2c.2). But, when DOX was released from the AuNPs, in acidic solution (Figure 2b.3), the fluorescence signal of DOX molecules was recovered (Figure 2c.3). It should be noted that AuNPs do not have any fluorescence emission in this region (Figure 2c.4). The Raman and fluorescence spectra demonstrated the plasmonic-tunable Raman/fluorescence properties of the DOX-AuNPs under different pHs, allowing "loaded" *versus* "released" states of DOX in relation to AuNPs to be tracked.

Raman/Fluorescence Properties of DOX-AuNPs in Living Cells. After confirming the principle of P-TRFIS, the Raman/fluorescence properties of DOX-AuNPs in human oral squamous carcinoma (HSC-3) cells were studied. The reported Raman spectra of live cell samples were the average of three independent experiments. At least 10 spectra were recorded from different cells in each

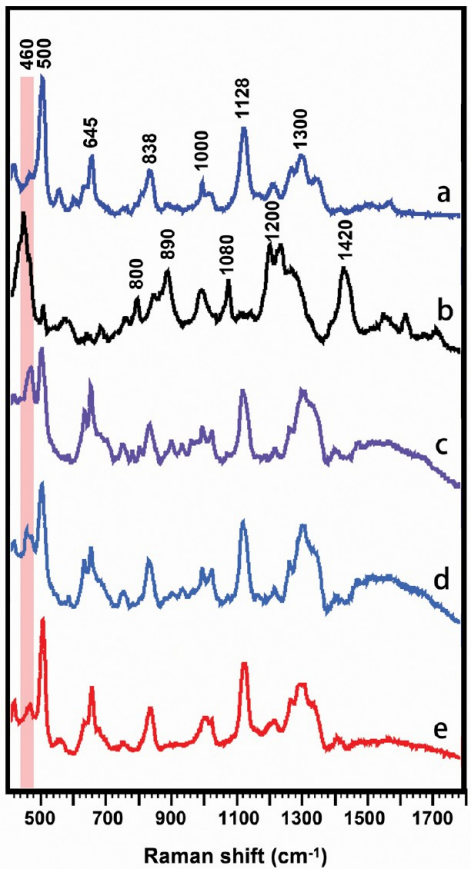

Figure 3. Raman spectra of control HSC-3 cells pretreated with 0.05 nM AuNPs (a), DOX-AuNPs alone (b), and HSC-3 cells incubated with 0.2 nM DOX-AuNPs for 3 h (c), 6 h (d), and 12 h (e).

experiment by using a 785 laser as the excitation source. Figure 3 shows the Raman spectra of control HSC-3 cells (a), DOX-AuNPs (b), and HSC-3 cells treated with 0.2 nM DOX-AuNPs for different periods of time (c—e). The control HSC-3 cells were pretreated with a low concentration (0.05 nM) of nuclear-targeted AuNPs to enhance the Raman signal without affecting the cell cycle or cell viability.[5] The control HSC-3 cells have characteristic bands at 500, 645, 838, 1000, 1128, and 1300 cm^{-1}, which correspond to the —S—S—, guanine and C—S, DNA backbone O—P—O, phenylalanine, peptide bond C—N, and amide III bands, respectively (Table 1).[8] The DOX-AuNPs have several Raman bands that are close to or overlapping with the bands of control HSC cells at 900—1500 cm^{-1} (Figure 3b). However, the strong, sharp band at 460 cm^{-1} is isolated from all the Raman bands of the drug bound to AuNPs while in HSC-3 cells. The Raman spectrum of HSC-3 cells treated with DOX-AuNPs for 3 h was similar to that of control HSC-3 cells, as the characteristic bands of HSC-3 cells were observed. The Raman features of DOX-AuNPs could not be distinguished in the spectrum, except for the strong, sharp band at 460 cm^{-1} (Figure 3c). This may be due to the overlap of the Raman features of DOX-AuNPs and HSC-3 cells as well

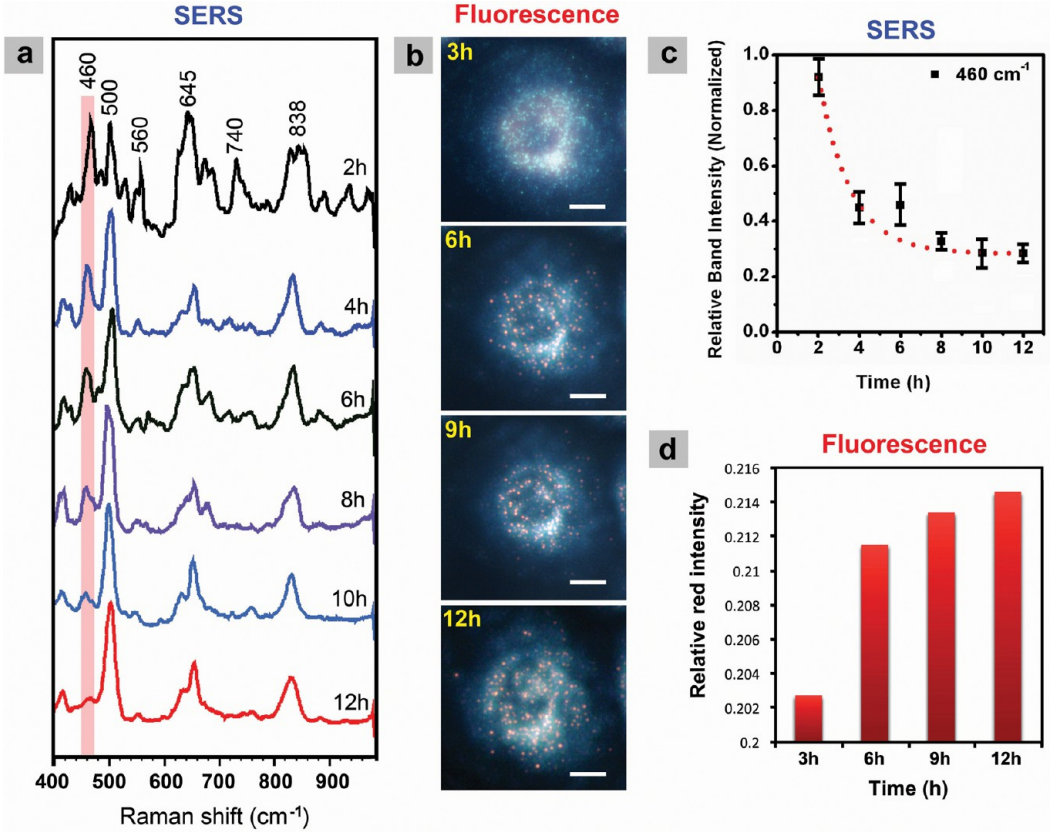

Figure 4. (a) Real-time monitoring of the drug release from AuNPs in HSC-3 cells by surface-enhanced Raman spectra; (b) fluorescence images of HSC-3 cells incubated with 0.2 nM DOX-AuNPs for different periods of time; the scale bar is 10 μm; (c) decrease of normalized Raman band intensities over time at 460 cm^{-1}; (d) increase of the relative intensity of red fluorescence in images over time.

as the strong Raman signal from the cells themselves. When the treatment time was increased to 6 and 12 h, the Raman band at 460 cm^{-1} continuously decreased, and the Raman spectrum resembled the spectroscopic features associated with control HSC-3 cells (Figure 3d and e). Therefore, the Raman band of DOX-AuNPs at 460 cm^{-1} was chosen as the band to monitor the release of DOX from gold nanoparticles, since it is sharp, strong, and separated from all other bands of the living cells.

Real-Time Study of DOX Release Dynamics in Living Cells. In order to monitor the release dynamics of DOX in real time, both Raman and fluorescence signals were recorded at different time points of drug treatment (Figure 4a and b). Figure 4a shows the Raman spectra of single living cells at different treatment times with 0.2 nM DOX-AuNPs. As stated above, due to the band overlap in the 1200−1600 cm^{-1} regions and the isolation of the 460 cm^{-1} band, we focused on monitoring the spectrum in the 400−1000 cm^{-1} region. When the HSC-3 cells were treated with 0.2 nM DOX-AuNPs for 2 h, the 460 cm^{-1} band was very strong. Additionally, the characteristic bands at 500, 645, and 838 cm^{-1}, which correspond to the −S−S−, C−S, and guanine, DNA backbone, respectively,[8] as well as several other bands at 560, 740, and 885 cm^{-1} were seen. These bands may be due to the spectra of DOX-AuNPs or the signals from cellular lipids and proteins.[28,29] The intensity of the 460 cm^{-1} band was found to decrease continuously at 4 h of DOX-AuNP incubation until it completely disappeared after 12 h of treatment (Figure 4c). This indicated that the DOX release from the AuNPs was time-dependent. To further confirm the results from the Raman spectra, we imaged HSC-3 cells treated with 0.2 nM DOX-AuNPs at different incubation periods using true-color fluorescence microscopy (Figure 4b). After 3 h of incubation, the functionalized nanoparticles were internalized through endocytosis, but no red fluorescence from DOX molecules was observed. This is attributed to the location of the DOX-AuNPs within the cell. At early stages of endocytosis, they are located in early endosomes, where the pH is not acidic enough to induce drug release (pH 6.5).[30] Thus, most of the fluorescence from DOX was quenched due to their proximity to the AuNPs' surface. At 6 h, the red fluorescence from DOX was observed within the cytoplasm. After 9 and 12 h of incubation, the intensity of the red fluorescence from DOX molecules increased within the cells, and the vessel-like red fluorescence spots were localized around the cell nucleus rather than being scattered within the cytoplasm. Figure 4d shows the relative intensity of the DOX red

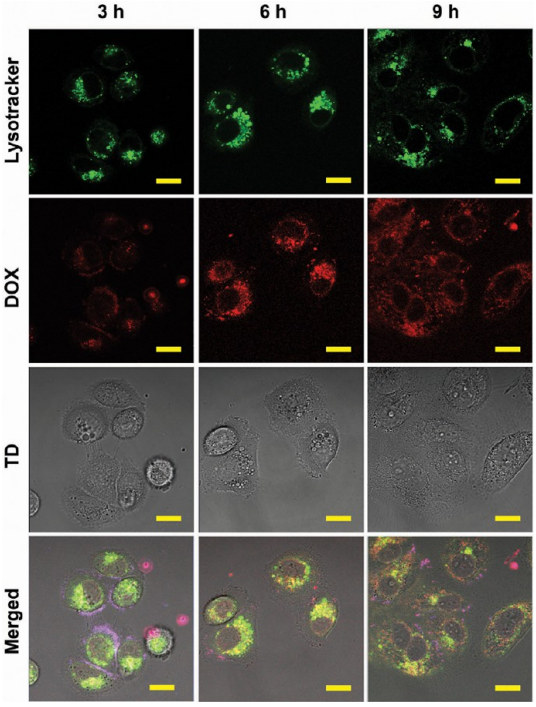

Figure 5. Multichannel confocal microscopy images of HSC-3 cells treated with 0.2 nM DOX-AuNPs after different incubation times. The lysosomes were stained by green LysoTracker, and the DOX is indicated by the red fluorescence. The scale bar is 20 μm.

fluorescence images at different times. The red fluorescence intensity increased in cells over time, indicating the continuous release of DOX molecules from AuNPs *via* hydrazone bond breakage induced by the slightly acidic pH microenvironment of the lysosomes (pH 5.0).

Co-localization of Lysosomal Activity and DOX Release. The investigation of the drug release mechanism induced by pH change was further conducted using a lysosome tracker fluorescent dye (green) that stains the cellular lysosomes (Figure 5). We studied the co-localization of DOX molecules within the lysosomes over time *via* multichannel confocal microscopy. After 3 h of treatment with 0.2 nM DOX-AuNPs, the red fluorescence (DOX) appeared on the cell membrane and inside the cytoplasm and not in the vicinity of the green-stained lysosomes. At the 6 h time point, the intensity of the red fluorescence increased and started to show co-localization with the green fluorescence of the labeled lysosomes. This is highly indicative of the DOX-AuNPs' translocation to the lysosomes and the subsequent DOX release as a result of the acidic microenvironment within the lysosomes. After 9 h of incubation, the intensity of the red fluorescence from DOX molecules had increased, and the red fluorescence appeared to be scattered throughout the entire cytoplasm rather than being localized within the green fluorescent lysosome regions. This scattered localization could be due to the lysosomal release of the DOX molecules and their subsequent diffusion into the cytoplasm.

CONCLUSION

We presented a plasmonic-tunable Raman/fluorescence imaging spectroscopy strategy to study the release of DOX drug molecules from gold nanoparticles in single living cells. The ability to utilize the plasmonic field of AuNPs to tune the Raman and fluorescence signals of DOX molecules enabled the Raman and fluorescence signals of DOX to be selectively switched "ON" and "OFF". This property allowed the DOX delivery and release process from AuNP carriers in a real-time manner on a single living cell level to be tracked. This technique has the potential to be a useful tool to study molecular mechanisms of drug delivery and release in living cells, as well as the cellular response to drug action. Further studies are currently being conducted to investigate the cytotoxicity and long-term cellular effects of DOX -functionalized AuNPs.

MATERIALS AND METHODS

AuNPs Synthesis. Citrate-stabilized AuNSs with an average diameter of 28 nm were synthesized by the reduction of chlorouric acid using sodium citrate. Briefly, 50 mL of 0.01% (by weight) auric acid (Sigma-Aldrich) aqueous solution was heated to boiling while stirring in a 100 mL beaker. Next, 1 mL of a 1% (by weight) trisodium citrate (Sigma-Aldrich) aqueous solution was added. Stirring and heating was stopped once a red wine color appeared. The solution was allowed to cool to room temperature. TEM images of the synthesized nanoparticles were taken by a JEOL 100CX transmission electron microscope. They showed an average diameter of 28 nm. UV–vis spectroscopy showed a peak surface plasmon resonance band at 531 nm.

AuNP PEG and Peptide Functionalization. Polyethylene glycol polymer was used to stabilize the nanoparticles to inhibit their aggregation during the drug–peptide conjugation. A 1.0 mM solution of PEG-SH (MW 5000, Laysan Bio, Inc.) dissolved in deionized (DI) water was added to the nanoparticle solution to achieve a mole ratio equivalent to 20% of the gold nanoparticle's surface (*ca.* 560 ligands per particle). The PEG-stabilized AuNS solution was allowed to shake at room temperature for 24 h, after which excess PEG was removed by centrifugation (4000*g*, 14 min). The washed PEG-AuNPs were redispersed in DI water. The PEGylated AuNPs were further conjugated with RGD and NLS peptides using a previously established method.[31] Briefly, a 5.0 mM NLS (GGVKRKKKPGGC) solution diluted in DI water and a 5.0 mM RGD (CGPDGRDGRDGRDGR) solution diluted in DI water were added to the PEG-conjugated particles to establish a mole ratio equivalent to 20% of the gold nanoparticle's surface (*ca.* 560 ligands per particle). The solution was allowed to shake at room temperature for 24 h, after which excess RGD and NLS were removed by centrifugation (4000*g*, 14 min). The washed AuNPs were redispersed in DI water and ready for DOX bioconjugation.

AuNP DOX Functionalization. The anticancer drug doxorubicin hydrochloride (Sigma-Aldrich, USA) was finally conjugated to the PEG-RGD-NLS nanoparticles with a pH-sensitive linker. To achieve that, we subjected the PEG-RGD-NLS-functionalized nanoparticles to methyl thioglyconate (MTG, Sigma-Aldrich, USA) and hydrazine (Sigma-Aldrich, USA). A 1.94 mM MTG solution dissolved in DI water was added to the AuNS to achieve a mole ratio equivalent to 40% of the gold nanoparticle's surface

(*ca*. 1131 added per particle). The nanoparticle solution was left to shake for 24 h, after which excess MTG was removed by centrifugation (4000*g*, 14 min). Hydrazine was then added to the PEG-RGD-MTG-functionalized nanoparticles. A 10 mM hydrazine solution dissolved in DI water was added to accomplish the same surface coverage as MTG. The nanoparticle solution was left under continuous stirring at 50 °C for 24 h. After washing the excess hydrazine by centrifugation (4000*g*, 14 min), DOX was finally added to bind to the hydrazine molecules *via* a hydrazone bond. A 1.73 mM solution of DOX was added to achieve the same surface coverage as hydrazine. The solution was left to shake at room temperature for 24 h. Excess DOX was removed, and the pellet was redispersed in DI water. The conjugation process was characterized by UV−vis spectroscopy. The DOX-conjugated AuNSs were dispersed in complete DMEM to the final required working concentration.

Cell Culture. HSC-3 (human oral squamous cell carcinoma), a malignant epithelial cell line expressing $\alpha_v\beta_6$ integrins on the cell membrane, was chosen as our cancer cell model.[32] The cell cultures were grown in Dulbecco's modified Eagle's complete medium (DMEM) (Mediatech) supplemented with 4.5 g/L glucose and sodium pyruvate, 10% v/v fetal bovine serum (FBS) (Mediatech), and 1% antimycotic solution (Mediatech). Cell cultures were kept at 37 °C in a 5% CO_2 humidified incubator.

Raman/Fluorescence Spectroscopy. The living cell Raman spectroscopy experiments were taken on a Renishaw InViva confocal Raman system combining dark field optics and a homemade living cell chamber, termed targeted plasmonically enhanced single cell imaging spectroscopy.[8] This system enables us to monitor the Rayleigh scattering cellular images and Raman scattering molecular spectral signals at the same time. For the spectra measurement, HSC-3 cells were cultured on 18 mm coverslips for 24 h in supplemented DMEM cell culture medium. Cells were then treated with designated concentrations of DOX-AuNPs for different periods of time. For the control cell group, the cells were incubated with 0.05 nM AuNSs for 24 h to enhance the Raman signals. When the incubation was done, the cell-containing coverslips were inserted into a homemade live cell chamber maintained at 37 °C and 5% CO_2 concentration. The chamber was then placed into the living cell Raman setup as demonstrated in our previous work.[8,33] Rayleigh and Raman spectra were obtained at different time points of DOX-AuNPs treatment. The Raman system utilized a 785 nm excitation laser, an inverted microscope with a 50× objective lens fitted with filters to exclude signals from the laser, and Rayleigh scattering. The presence of AuNPs enabled the acquisition of well-resolved spectra to be under 10 s when using the extended scan mode. The static mode required <1 s. For each time point, at least 10 spectra were taken from different individual cells, and three independent experiments were used to obtain averaged Raman data, which were then normalized to the most intense band. The Raman spectra of the DOX, AuNPs, and DOX-AuNPs in solution were recorded on the same system by using the same homemake fluidic chamber.

The living cell fluorescence microscopy experiments were done with the same T-PESCIS system by adding new fluorescence optics. The final combined system was named plasmonic-tunable Raman/fluorescence imaging spectroscopy. A halogen lamp was used as excitation light; a 500 nm short pass filter was used as an excitation filter. The fluorescence signals were then passed through a 520 nm long-pass dichromatic mirror and collected by a CCD camera.

The fluorescence spectra of the gold nanoparticle solution were taken on a PTI model C60 steady-state spectrofluorometer using a xenon arc lamp source and a photomultiplier detection system.

Confocal Imaging. LysoTracker green DND-2 6 (Molecular Probes, USA), a cell-permeable green dye, was used to stain the acidic compartments (lysosomes) in live cells. Briefly, HSC-3 cells were cultured on 35 mm glass-bottom dishes (MatTeck, USA) in cell culture medium (DMEM) for 24 h. After that, cells were treated with 0.2 nM DOX-AuNPs and incubated for the desired time frame. At the designated time point, the particle-containing cell culture medium was removed, the cells were washed twice with PBS, and a fresh probe-containing medium was added at a final concentration of 50 nM. The cells were incubated for an additional 30 min at 37 °C in a 5% CO_2 humidified incubator. After that, the cells were washed with PBS, and a fresh complete clear medium was added. Finally, live cells stained with the dye were visualized using a Zeiss LSM700-405 confocal microscope.

Conflict of Interest: The authors declare no competing financial interest.

Supporting Information Available: TEM and UV−vis data of AuNPs are included. This material is available free of charge *via* the Internet at http://pubs.acs.org.

Acknowledgment. The authors would like to acknowledge Georgia Institute of Technology for supporting the research.

REFERENCES AND NOTES

1. Huang, W.; Qian, W.; El-Sayed, M. A. Gold Nanoparticles Propulsion from Surface Fueled by Absorption of Femtosecond Laser Pulse at Their Surface Plasmon Resonance. *J. Am. Chem. Soc.* **2006**, *128*, 13330–13331.
2. Huang, X. H.; El-Sayed, I. H.; Qian, W.; El-Sayed, M. A. Cancer Cell Imaging and Photothermal Therapy in the Near-Infrared Region by Using Gold Nanorods. *J. Am. Chem. Soc.* **2006**, *128*, 2115–2120.
3. Dreaden, E. C.; Mackey, M. A.; Huang, X. H.; Kang, B.; El-Sayed, M. A. Beating Cancer in Multiple Ways Using Nanogold. *Chem. Soc. Rev.* **2011**, *40*, 3391–3404.
4. Dreaden, E. C.; Alkilany, A. M.; Huang, X. H.; Murphy, C. J.; El-Sayed, M. A. The Golden Age: Gold Nanoparticles for Biomedicine. *Chem. Soc. Rev.* **2012**, *41*, 2740–2779.
5. Kang, B.; Mackey, M. A.; El-Sayed, M. A. Nuclear Targeting of Gold Nanoparticles in Cancer Cells Induces DNA Damage, Causing Cytokinesis Arrest and Apoptosis. *J. Am. Chem. Soc.* **2010**, *132*, 1517–1519.
6. Qian, W.; Huang, X. H.; Kang, B.; El-Sayed, M. A. Dark-Field Light Scattering Imaging of Living Cancer Cell Component from Birth through Division Using Bioconjugated Gold Nanoprobes. *J. Biomed. Opt.* **2010**, *15*, 046025.
7. Austin, L. A.; Kang, B.; Yen, C. W.; El-Sayed, M. A. Plasmonic Imaging of Human Oral Cancer Cell Communities during Programmed Cell Death by Nuclear-Targeting Silver Nanoparticles. *J. Am. Chem. Soc.* **2011**, *133*, 17594–17597.
8. Kang, B.; Austin, L. A.; El-Sayed, M. A. Real-Time Molecular Imaging throughout the Entire Cell Cycle by Targeted Plasmonic-Enhanced Rayleigh/Raman Spectroscopy. *Nano Lett.* **2012**, *12*, 5369–5375.
9. Timko, B. P.; Dvir, T.; Kohane, D. S. Remotely Triggerable Drug Delivery Systems. *Adv. Mater.* **2010**, *22*, 4925–4943.
10. Thomas, C. R.; Ferris, D. P.; Lee, J. H.; Choi, E.; Cho, M. H.; Kim, E. S.; Stoddart, J. F.; Shin, J. S.; Cheon, J.; Zink, J. I. Noninvasive Remote-Controlled Release of Drug Molecules in *Vitro* Using Magnetic Actuation of Mechanized Nanoparticles. *J. Am. Chem. Soc.* **2010**, *132*, 10623–10625.
11. Khashab, N. M.; Belowich, M. E.; Trabolsi, A.; Friedman, D. C.; Valente, C.; Lau, Y. N.; Khatib, H. A.; Zink, J. I.; Stoddart, J. F. pH-Responsive Mechanised Nanoparticles Gated by Semirotaxanes. *Chem. Commun.* **2009**, 5371–5373.
12. Vivero-Escoto, J. L.; Slowing, I. I.; Wu, C. W.; Lin, V. S. Y. Photoinduced Intracellular Controlled Release Drug Delivery in Human Cells by Gold-Capped Mesoporous Silica Nanosphere. *J. Am. Chem. Soc.* **2009**, *131*, 3462–3463.
13. Rai, P.; Mallidi, S.; Zheng, X.; Rahmanzadeh, R.; Mir, Y.; Elrington, S.; Khurshid, A.; Hasan, T. Development and Applications of Photo-Triggered Theranostic Agents. *Adv. Drug Delivery Rev.* **2010**, *62*, 1094–1124.
14. Choi, S. W.; Zhang, Y.; Xia, Y. N. A Temperature-Sensitive Drug Release System Based on Phase-Change Materials. *Angew. Chem., Int. Ed.* **2010**, *49*, 7904–7908.
15. Yavuz, M. S.; Cheng, Y. Y.; Chen, J. Y.; Cobley, C. M.; Zhang, Q.; Rycenga, M.; Xie, J. W.; Kim, C.; Song, K. H.; Schwartz, A. G.; *et al.* Gold Nanocages Covered by Smart Polymers for Controlled Release with Near-Infrared Light. *Nat. Mater.* **2009**, *8*, 935–939.

16. Aryal, S.; Grailer, J. J.; Pilla, S.; Steeber, D. A.; Gong, S. Q. Doxorubicin Conjugated Gold Nanoparticles as Water-Soluble and pH-Responsive Anticancer Drug Nanocarriers. *J. Mater. Chem.* **2009**, *19*, 7879–7884.
17. Kimling, J.; Maier, M.; Okenve, B.; Kotaidis, V.; Ballot, H.; Plech, A. Turkevich Method for Gold Nanoparticle Synthesis Revisited. *J. Phys. Chem. B* **2006**, *110*, 15700–15707.
18. Takayama, S.; Hatori, M.; Kurihara, Y.; Kinugasa, Y.; Shirota, T.; Shintani, S. Inhibition of Tgf-Beta 1 Suppresses Motility and Invasiveness of Oral Squamous Cell Carcinoma Cell Lines *via* Modulation of Integrins and Down-Regulation of Matrix-Metalloproteinases. *Oncol. Rep.* **2009**, *21*, 205–210.
19. Xue, H.; Atakilit, A.; Zhu, W. M.; Li, X. W.; Ramos, D. M.; Pytela, R. Role of the Alpha V Beta 6 Integrin in Human Oral Squamous Cell Carcinoma Growth in *Vivo* and in *Vitro*. *Biochem. Biophys. Res. Commun.* **2001**, *288*, 610–618.
20. Dingwall, C.; Laskey, R. A. Nuclear Targeting Sequences-A Consensus. *Trends Biochem. Sci.* **1991**, *16*, 478–481.
21. Robbins, J.; Dilworth, S. M.; Laskey, R. A.; Dingwall, C. 2 Interdependent Basic Domains in Nucleoplasmin Nuclear Targeting Sequence - Identification of a Class of Bipartite Nuclear Targeting Sequence. *Cell* **1991**, *64*, 615–623.
22. Dulkeith, E.; Morteani, A. C.; Niedereichholz, T.; Klar, T. A.; Feldmann, J.; Levi, S. A.; van Veggel, F. C. J. M.; Reinhoudt, D. N.; Moller, M.; Gittins, D. I. Fluorescence Quenching of Dye Molecules near Gold Nanoparticles: Radiative and Nonradiative Effects. *Phys. Rev. Lett.* **2002**, *89*, 203002.
23. Li, J. F.; Huang, Y. F.; Ding, Y.; Yang, Z. L.; Li, S. B.; Zhou, X. S.; Fan, F. R.; Zhang, W.; Zhou, Z. Y.; Wu, D. Y.; *et al*. Shell-Isolated Nanoparticle-Enhanced Raman Spectroscopy. *Nature* **2010**, *464*, 392–395.
24. Schneider, G.; Decher, G.; Nerambourg, N.; Praho, R.; Werts, M. H. V.; Blanchard-Desce, M. Distance-Dependent Fluorescence Quenching on Gold Nanoparticles Ensheathed with Layer-by-Layer Assembled Polyelectrolytes. *Nano Lett.* **2006**, *6*, 530–536.
25. Lee, C. J.; Kang, J. S.; Kim, M. S.; Lee, K. P.; Lee, M. S. The Study of Doxorubicin and Its Complex with DNA by SERS and UV-Resonance Raman Spectroscopy. *Bull. Korean Chem. Soc.* **2004**, *25*, 1211–1216.
26. Eliasson, C.; Loren, A.; Murty, K. V. G. K.; Josefson, M.; Kall, M.; Abrahamsson, J.; Abrahamsson, K. Multivariate Evaluation of Doxorubicin Surface-Enhanced Raman Spectra. *Spectrochim. Acta. A* **2001**, *57*, 1907–1915.
27. Loren, A.; Eliasson, C.; Josefson, M.; Murty, K. V. G. K.; Kall, M.; Abrahamsson, J.; Abrahamsson, K. Feasibility of Quantitative Determination of Doxorubicin with Surface-Enhanced Raman Spectroscopy. *J. Raman Spectrosc.* **2001**, *32*, 971–974.
28. Van Manen, H. J.; Kraan, Y. M.; Roos, D.; Otto, C. Single-Cell Raman and Fluorescence Microscopy Reveal the Association of Lipid Bodies with Phagosomes in Leukocytes. *Proc. Natl. Acad. Sci. U.S.A.* **2005**, *102*, 10159–10164.
29. Wu, H. W.; Volponi, J. V.; Oliver, A. E.; Parikh, A. N.; Simmons, B. A.; Singh, S. *In Vivo* Lipidomics Using Single-Cell Raman Spectroscopy. *Proc. Natl. Acad. Sci. U.S.A.* **2011**, *108*, 3809–3814.
30. Jovic, M.; Sharma, M.; Rahajeng, J.; Caplan, S. The Early Endosome: A Busy Sorting Station for Proteins at the Crossroads. *Histol. Histopathol.* **2010**, *25*, 99–112.
31. Austin, L. A.; Kang, B.; Yen, C. W.; El-Sayed, M. A. Nuclear Targeted Silver Nanospheres Perturb the Cancer Cell Cycle Differently Than Those of Nanogold. *Bioconjugate Chem.* **2011**, *22*, 2324–2331.
32. Oyelere, A. K.; Chen, P. C.; Huang, X. H.; El-Sayed, I. H.; El-Sayed, M. A. Peptide-Conjugated Gold Nanorods for Nuclear Targeting. *Bioconjugate Chem.* **2007**, *18*, 1490–1497.
33. Austin, L. A.; Kang, B.; El-Sayed, M. A. A New Nanotechnology Technique for Determining Drug Efficacy Using Targeted Plasmonically Enhanced Single Cell Imaging Spectroscopy. *J. Am. Chem. Soc.* **2013**, *135*, 4688–4691.